THE ARCHIVE OF MECHANICAL ENGINEERING

Vol. XLVIII 2001 Number 4

Key words: *turboshaft engine, compressor, surge margin*

STANISŁAW ANTAS[*)]

AN ANALYTICAL AND NUMERICAL METHOD OF CALCULATING THE SURGE MARGIN OF COMPRESSOR OF TURBOSHAFT ENGINE WITH FREE POWER TURBINE

This paper presents description of the comprehensive computational analysis aimed at providing compressor stable operation range. In this article the author presents the computational predictions of compressor surge margin value, derived by means of originally elaborated analytical and numerical methods. One has defined, in both analytical and numerical way, the influence of change of throat area of gasifier turbine nozzle guide vanes $(F_{GV})_{CT}$, and change of throat area of power turbine nozzle guide vanes $(F_{GV})_{PT}$ on engine compressor surge margin measured in manufacturing condition with the value of π_C^*/G_{1cor} ratio. The results of computational analysis are compared with measured parameters obtained from experimental tests of turboshaft engine. Conclusions from the computational analyses are then presented.

Nomenclature

A – mass flow parameter,
c – absolute velocity,
F – section area,
G – mass flow rate,
k – isentropic constant,
K – stable running factor,
l – specific work,
m_g – polytropic exponent for combustion gas,
n – rotational speed,
N – power,
p_i^* – stagnation pressure in a given control section,
R – gas constant,
s_{fg} – continuity equation constant for combustion gas,

*) *Transport Equipment Enterprise „PZL-Rzeszów" S.A.; ul. Hetmańska 120, 35-078 Rzeszów, Poland; E-mail: eantas@prz.rzeszow.pl*

T_i^* – stagnation temperature in a given control section,
β – correction coefficient,
η – efficiency,
λ – Laval number,
μ – flow rate coefficient,
π – compression ratio of compressor, or expansion ratio of turbine,
ρ – density,
σ – recovery factor of total pressure,
$q(\lambda)$ – mass flux density, $c\rho / c_{crit}\rho_{crit}$.

Subscripts and superscripts

/* – stagnation,
/*IN* – intake,
/*C* – compressor,
/*B* – combustion chamber,
/*CT* –compressor turbine,
/*PT* – power turbine,
/*D* – exhaust diffuser,
/*GV* – nozzle vane,
/*a* – air,
/*g* – gas,
/*crit* – critical value,
/*cor* – corrected,
/*sl* – compressor surge line,
/1, 2,...6 – control sections,

1. Introduction

The operational ratings of an aviation turboshaft engine are bounded on the compressor performance map by the surge limit and choke lines. The surge line separates the regions of stable and unstable compressor operation. Unstable operation results in repeating fluctuations of air flow consisting in accumulation and downstream flow to the engine inlet. Consequently, pressure and mass flow rate change violently.

Simultaneously, the medium pressure on compressor outlet, its compression ratio and efficiency considerably decrease. The gas temperature on turbine inlet increases and engine power violently decreases [14]. If, moreover, the frequency of pressure fluctuations coincide with free vibration frequency of compressor components, this phenomenon may quickly lead to compressor damage. Thus, the surge line of a compressor shall not be exceeded in any engine operational conditions [16].

To avoid these serious consequences, the compressor working line must be far enough from the surge line. Quantitative estimation of the distance of steady-

state operating line from the surge line for chosen corrected speed curve $n_{Ccor} = \text{idem}$ can be done by means of the compressor stable running factor determined by the formula [2]

$$K_C = \frac{\pi^*_{Csl}/(G_{1cor})_{sl}}{\pi^*_C/G_{1cor}}, \tag{1}$$

and the surge margin of compressor ΔK_C is defined by

$$\Delta K_C = K_C - 1, \tag{2}$$

or

$$\Delta K_{C\%} = (K_C - 1)\cdot 100, \ \% \tag{3}$$

where G_{1cor} and $(G_{1cor})_{sl}$ are corrected mass flow rates (mass stream) of air determined at the compressor inlet at the working point and at the surge line suitably for $n_{Ccor} = \text{idem}$, whereas, π^*_C, π^*_{Csl} is a compressor ratio.

In manufacturing conditions, the value of surge margin of compressor (ΔK_C) of the PZL-10W aviation turbine engine with a free power turbine (Fig. 1) is determined by a change of throat area of gasifier turbine nozzle guide vanes $(F_{GV})_{CT}$ and a change of throat area of power turbine nozzle guide vanes $(F_{GV})_{PT}$ [2].

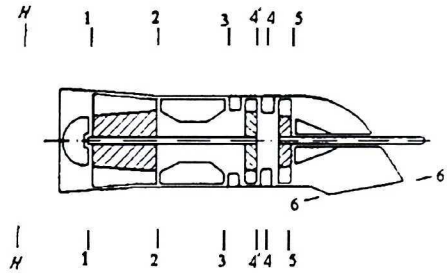

Fig. 1. Designation of control planes of turboshaft engine with free power turbine

These changes influence decisively the location of the C-CT working line on the compressor map, thus, on the compressor surge margin ΔK_C [2]. According to what was mentioned above, complete analysis of the effect of $(F_{GV})_{CT}$ and $(F_{GV})_{PT}$ on ΔK_C change requires that calculation methods are used, making it possible to find the compressor surge margin for both engine design regime (when $n_{Ccor} = \text{idem}$) and other regimes (when $n_{Ccor} = \text{var}$).

Unfortunately, there are not any methods described in detail published in the available literature. This compelled us to elaborate our own method of numerical and analytical calculations.

It should be stated that problems connected with theoretical and experimental analysis of phenomena taking place in a compressor during unstable compressor operation and conditions of its stable operation have been the subject of interest in by many research centres for a long time [8], [10], [12], [13], [17]. Many of

authors have been seriously interested in these problems in recent years [14], [16], [19].

2. Analytical method

In the case when inappropriate value of the criterion π_C^* / G_{1cor} (ie., inappropriate value of ΔK_C) is obtained during acceptance test of an engine, it is required to dismount the engine turbines, as well as to select the throat areas of gasifier and power turbine nozzle guide vanes $(F_{GV})_{CT}$ and $(F_{GV})_{PT}$. A designer, who selects a proper set of $(F_{GV})_{CT}$ and $(F_{GV})_{PT}$ needs to use a quick, analytical method, ie. relations that enable him to find ΔK_C for chosen configuration of the throat areas. To solve this essential problem, in practical terms, one used the main instrument facilitating the analysis of changes of working medium stream parameters that occurred because of aerodynamic action of engine flow channels, namely – gas dynamics conservation equations [5].

The analytical procedure of finding function of the compressor surge margin for the changes of the throat areas of gasifier and power turbine nozzle guide vanes is as follows.

Taking into account the relation (1) and formula (3), one may write

$$\Delta K_{C\%} = \left[\frac{\pi_{Csl}^*}{(G_{1cor})_{sl}} \frac{G_{1cor}}{\pi_C^*} - 1 \right] \cdot 100 , \tag{4}$$

from where, in general:

$$\frac{\Delta K_{C\%}}{100} + 1 = \frac{\pi_{Csl}^*}{(G_{1cor})_{sl}} \frac{G_{1cor}}{\pi_C^*} . \tag{5}$$

For a chosen compressor characteristic branch, $n_{Ccor} = \text{idem}$, the co-ordinates of the surge limit point comply to the relation

$$\frac{\pi_{Csl}^*}{(G_{1cor})_{sl}} = \text{idem} . \tag{6}$$

According to theoretical analysis of the increase of compressor surge margin caused by the change of C-CT working line position, one may write for the point a' corresponding to compressor parameters obtained for the throat area of gasifier turbine nozzle guide vanes $(F_{GV})_{CT}'$

$$\frac{\Delta K'_{C\%}}{100} = \frac{\pi_{Csl}^*}{(G_{1cor})_{sl}} \frac{G'_{1cor}}{\pi_C^{*'}} - 1 , \tag{7}$$

and for the point a''

$$\frac{\Delta K''_{C\%}}{100} = \frac{\pi_{Csl}^*}{(G_{1cor})_{sl}} \frac{G'_{1cor}}{\pi_C^{*''}} - 1 . \tag{8}$$

Thus, the increase of the compressor surge margin value produced by the change of C-CT working line position is as below

$$\frac{\delta(\Delta K_{C\%})}{100} = \frac{\Delta K''_{C\%}}{100} - \frac{\Delta K'_{C\%}}{100}, \tag{9}$$

while, taking into consideration the formulas (7) and (8) one may write:

$$\frac{\delta(\Delta K_{C\%})}{100} = \left(\frac{\Delta K'_{C\%}}{100} + 1\right)\left(\frac{G''_{1cor}/\pi_C^{*''}}{G'_{1cor}/\pi_C^{*'}} - 1\right). \tag{10}$$

General relation characterising the quotient of compressor inlet air mass flow to pressure ratio in the formula (10) is found from the equation of continuity written for the flow between compressor inlet section and minimal section of compressor turbine nozzle rim [2]

$$(G_{GV})_{CT} = \beta G_1 = s_{fg}\frac{p^*_{GV}}{\sqrt{T^*_{GV}}}(F_{GV})_{CT}\, q(\lambda_{GV})_{CT}\, \mu_{GVCT}, \tag{11}$$

where $p^*_{GV} = p^*_2 \sigma_B \sigma_{GVCT}$,

$T^*_{GV} = T^*_3$,

but

$$p^*_2 = \pi^*_C p^*_H \sigma_{IN} \tag{12}$$

therefore

$$p^*_{GV} = \pi^*_C p^*_H \sigma_{IN} \sigma_B \sigma_{GVCT}, \tag{13}$$

thus, having substituted the formula (13) to the relation (10) one receives

$$G_1 = s_{fg}\frac{\pi^*_C p^*_H \sigma_{IN}\sigma_B\sigma_{GVCT}}{\beta\sqrt{T^*_3}}(F_{GV})_{CT}\, q(\lambda_{GV})_{CT}\, \mu_{GVCT}, \tag{14}$$

from where

$$\frac{G_1}{\pi^*_C} = s_{fg}\frac{p^*_H \sigma_{IN}\sigma_B\sigma_{GVCT}}{\beta\sqrt{T^*_3}}(F_{GV})_{CT}\, q(\lambda_{GV})_{CT}\, \mu_{GVCT}. \tag{15}$$

Suitably, for the a' and a'' point on the compressor map, the following is obtained

$$\frac{G'_1}{\pi_C^{*'}} = s_{fg}\frac{p^*_H \sigma_{IN}\sigma_B\sigma_{GVCT}}{\beta\sqrt{T_3^{*'}}}(F_{GV})'_{CT}\, q(\lambda_{GV})'_{CT}\, \mu_{GVCT}, \tag{16}$$

and

$$\frac{G''_1}{\pi_C^{*''}} = s_{fg}\frac{p^*_H\, \sigma_{IN}\sigma_B\, \sigma_{GVCT}}{\beta\sqrt{T_3^{*''}}}(F_{GV})''_{CT}\, q(\lambda_{GV})''_{CT}\, \mu_{GVCT}. \tag{17}$$

Dividing the formulas (17) and (16) by themselves, one may write

$$\frac{G''_1/\pi_C^{*''}}{G'_1/\pi_C^{*'}} = \frac{q(\lambda_{GV})''_{CT}}{q(\lambda_{GV})'_{CT}}\sqrt{\frac{T_3^{*'}}{T_3^{*''}}}\frac{(F_{GV})''_{CT}}{(F_{GV})'_{CT}}. \tag{18}$$

Introducing an additional relation

$$(F_{GV})''_{CT} = (F_{GV})'_{CT} + \Delta(F_{GV})_{CT}, \tag{19}$$

one may have

$$\frac{G_1^{''}/\pi_C^{*''}}{G_1^{'}/\pi_C^{*'}}=\frac{q(\lambda_{GV})_{CT}^{''}}{q(\lambda_{GV})_{CT}^{'}}\sqrt{\frac{T_3^{*'}}{T_3^{*''}}}\left[1+\frac{\Delta(F_{GV})_{CT}}{(F_{GV})_{CT}^{'}}\right]. \tag{20}$$

For speed $n_{Ccor}=\text{idem}$ chosen on the compressor map, it may be written

$$\frac{q(\lambda_{GV})_{CT}^{''}}{q(\lambda_{GV})_{CT}^{'}}\sqrt{\frac{T_3^{*'}}{T_3^{*''}}}\approx 1. \tag{21}$$

Taking into account the formula (21), the relation (20) is as follows

$$\frac{G_1^{''}/\pi_C^{*''}}{G_1^{'}/\pi_C^{*'}}=1+\frac{\Delta(F_{GV})_{CT}}{(F_{GV})_{CT}^{'}}, \tag{22}$$

from where

$$\frac{G_1^{''}}{\pi_C^{*''}}=\frac{G_1^{'}}{\pi_C^{*'}}\left[1+\frac{\Delta(F_{GV})_{CT}}{(F_{GV})_{CT}^{'}}\right], \tag{23}$$

and

$$\frac{\pi_C^{*''}}{G_1^{''}}=\frac{\pi_C^{*'}}{G_1^{'}}\left[\frac{1}{1+\dfrac{\Delta(F_{GV})_{CT}}{(F_{GV})_{CT}^{'}}}\right]. \tag{24}$$

The mentioned above relations are also valid for compressor reduced parameters, because

$$G_1=G_{1cor}\frac{p_H^*}{1.01325\cdot 10^5}\sqrt{\frac{288.15}{T_H^*}}, \tag{25}$$

or

$$G_1=G_{1cor}\frac{p_H^*}{1.01325\cdot 10^5}\frac{n_{Ccor}}{n_C}. \tag{26}$$

The increase of the criterion value π_C^*/G_{1cor} characterising the compressor surge margin

$$\Delta\left(\frac{\pi_C^*}{G_{1cor}}\right)=\frac{\pi_C^{*''}}{G_{1cor}^{''}}-\frac{\pi_C^{*'}}{G_{1cor}^{'}}, \tag{27}$$

may be easily determined by using formula (24), since

$$\Delta\left(\frac{\pi_C^*}{G_{1cor}}\right)=\frac{\pi_C^{*'}}{G_{1cor}^{'}}\left[\frac{1}{1+\dfrac{\Delta(F_{GV})_{CT}}{(F_{GV})_{CT}^{'}}}-1\right]. \tag{28}$$

Next, substituting formula (22) for relation (10), finally allows us to determine the relation

$$\frac{\delta(\Delta K_{C\%})}{100}=\left(\frac{\Delta K'_{C\%}}{100}+1\right)\frac{\Delta(F_{GV})_{CT}}{(F_{GV})'_{CT}}. \tag{29}$$

The function of the compressor surge margin versus the change of the minimal section of power turbine nozzle rim may be determined by analysing the continuity equation written for this rim (30)

$$(G_{GV})_{PT}=s_{fg}\frac{p_4^*}{\sqrt{T_4^*}}(F_{GV})_{PT}\,q(\lambda_{GV})_{PT}\,\sigma_{GVPT}\mu_{GVPT}. \tag{30}$$

This formula may be rearranged by taking into consideration the relation of combustion gas mass stream entering the power turbine against air mass flow rate at the compressor inlet [2]

$$(G_{GV})_{PT}=(\beta+\delta_{PT})G_1 \tag{31}$$

and the relation

$$p_4^*=p_4^{*}\,\sigma_{MT}$$

where, from the formula defining the pressure ratio of compressor turbine one has

$$p_4^{*}=\frac{p_3^*}{\pi_{CT}^*}. \tag{32}$$

On the other hand, the stagnation pressure at the combustion chamber outlet may be as follows

$$p_3^*=p_2^*\sigma_B^*=p_1^*\pi_C^*\sigma_B^*. \tag{33}$$

Next, the stagnation pressure at the compressor entry is defined by

$$p_1^*=p_H^*\sigma_{IN}. \tag{34}$$

Taking into consideration the relation mentioned above, the stagnation pressure at the power turbine entry may be written as

$$p_4^*=\frac{p_H^*\sigma_{IN}\pi_C^*\sigma_B\sigma_{MT}}{\pi_{CT}^*}. \tag{35}$$

Thus, one may re-write equation (30) as

$$G_1(\beta+\delta_{PT})=s_{fg}\frac{p_H^*\;\sigma_{IN}\pi_C^*\;\sigma_B\sigma_{MT}\,(F_{GV})_{PT}\;q(\lambda_{GV})_{PT}\,\sigma_{GVPT}\,\mu_{GVPT}}{\sqrt{T_4^*}\;\;\pi_{CT}^{*\;\frac{2m_g}{m_g+1}}} \tag{36}$$

From relation (36), one can easily obtain a general form of the quotient of compressor inlet flow rate to the value of compressor pressure ratio

$$\frac{G_1}{\pi_C^*}=s_{fg}\frac{p_H^*\sigma_{IN}\sigma_B\sigma_{MT}\,(F_{GV})_{PT}\,q(\lambda_{GV})_{PT}\,\sigma_{GVPT}\,\mu_{GVPT}}{(\beta+\delta_{PT})\sqrt{T_4^*}\;\pi_{CT}^{*\;\frac{2m_g}{m_g+1}}}. \tag{37}$$

Suitably, for points a' and a'' of the compressor map, one obtains the following

$$\frac{G_1'}{\pi_C^{*'}} = s_{fg} \frac{p_H^* \ \sigma_{IN}\sigma_B\sigma_{MT} \left(F_{GV}\right)_{PT}' q\left(\lambda_{GV}\right)_{PT}' \sigma_{GVPT}\mu_{GVPT}}{(\beta+\delta_{PT})\sqrt{T_4^{*'}}\ \pi_{CT}^{*'\ \frac{2m_g}{m_g+1}}}, \tag{38}$$

and

$$\frac{G_1''}{\pi_C^{*''}} = s_{fg} \frac{p_H^* \ \sigma_{IN}\sigma_B\sigma_{MT} \left(F_{GV}\right)_{PT}'' q\left(\lambda_{GV}\right)_{PT}'' \sigma_{GVPT}\mu_{GVPT}}{(\beta+\delta_{PT})\sqrt{T_4^{*''}}\ \pi_{CT}^{*''\ \frac{2m_g}{m_g+1}}}. \tag{39}$$

Dividing formulas (39) and (38) by sides, one may write

$$\frac{G_1''/\pi_C^{*''}}{G_1'/\pi_C^{*'}} = \frac{\left(F_{GV}\right)_{PT}''\ q\left(\lambda_{GV}\right)_{PT}''\ \sqrt{T_4^{*'}}\ \pi_{CT}^{*'\ \frac{2m_g}{m_g+1}}}{\left(F_{GV}\right)_{PT}'\ q\left(\lambda_{GV}\right)_{PT}'\ \sqrt{T_4^{*''}}\ \pi_{CT}^{*''\ \frac{2m_g}{m_g+1}}}. \tag{40}$$

For a n_{Ccor} = idem speed chosen from the compressor map, one may assume

$$\frac{\sqrt{T_4^{*'}}\ \pi_{CT}^{*'\ \frac{2m_g}{m_g+1}}}{\sqrt{T_4^{*''}}\ \pi_{CT}^{*''\ \frac{2m_g}{m_g+1}}} \approx 1, \tag{41}$$

while, for critical and supercritical power turbine pressure ratios there is

$$q\left(\lambda_{GV}\right)_{PT}' = q\left(\lambda_{GV}\right)_{PT}'' = 1. \tag{42}$$

Taking into consideration equations (41) and (42), relation (40) may be written as

$$\frac{G_1''/\pi_C^{*''}}{G_1'/\pi_C^{*'}} = \frac{\left(F_{GV}\right)_{PT}''}{\left(F_{GV}\right)_{PT}'}. \tag{43}$$

Additionally, considering the following formula

$$\left(F_{GV}\right)_{PT}'' = \left(F_{GV}\right)_{PT}' + \Delta\ \left(F_{GV}\right)_{PT}, \tag{44}$$

one obtains

$$\frac{G_1''/\pi_C^{*''}}{G_1'/\pi_C^{*'}} = 1 + \frac{\Delta\ \left(F_{GV}\right)_{PT}}{\left(F_{GV}\right)_{PT}'}, \tag{45}$$

from where

$$\frac{G_1''}{\pi_C^{*''}} = \frac{G_1}{\pi_C^{*'}}\left[1 + \frac{\Delta\ \left(F_{GV}\right)_{PT}}{\left(F_{GV}\right)_{PT}'}\right], \tag{46}$$

and

$$\frac{\pi_C^{*''}}{G_1''} = \frac{\pi_C^{*'}}{G_1'}\left[\frac{1}{1+\dfrac{\Delta\left(F_{GV}\right)_{PT}}{\left(F_{GV}\right)_{PT}'}}\right]. \tag{47}$$

The increase of π_C^* / G_{1cor} criterion that characterises the compressor surge margin (eq. 27) as a function of the minimal section area of power turbine guide vanes, may be found from relation (47), because

$$\Delta\left(\frac{\pi_C^*}{G_{1cor}}\right) = \frac{\pi_C^{*'}}{G_{1cor}'}\left[\frac{1}{1+\dfrac{\Delta\left(F_{GV}\right)_{PT}}{\left(F_{GV}\right)_{PT}'}} - 1\right]. \tag{48}$$

Whereas, by substituting formula (45) to equation (10) one finds an explicit function that describes the increment of compressor surge margin value related to the change of minimal section area of power turbine guide vanes

$$\frac{\delta\left(\Delta K_{C\%}\right)}{100} = \left(\frac{\Delta K_{C\%}'}{100} + 1\right)\frac{\Delta\left(F_{GV}\right)_{PT}}{\left(F_{GV}\right)_{PT}'}. \tag{49}$$

The equations (28), (29) and (48), (49) make it possible to find directly an analytical definition for the influence of change of minimal section area of compressor and power turbine guide vanes on the change of value of compressor surge margin [5].

3. Numerical method

A turboshaft engine represents a complex system that comprises a number of rotating and stationary components, each having its own performance characteristics. The performance of the complete engine depends on the performance characteristics of the individual components or subsystems and component matching. Moreover, in the service, an engine is operated over a wide range of flight conditions.

Hence, testing a complete engine to explore its full performance envelope can be both very costly and extremely laborious. Therefore, simulating the operation of the aviation gas turbine engine on a computer has obvious advantages. The aim of this section is to describe a general simulation model, which has been used for OST microcomputer-based program. This program has been applied for digital simulation of steady-state performance of turboshaft engine with free power turbine.

At stable running conditions of compressor and gasifier turbine, the location of steady-state operating line C-CT (also called the working or operating line)

depends on the operating range of the engine and on the methods of its control. Generally, the working line points are geometric locus of points resulting from the function

$$Y = f\left(\pi_C^*, G_{1cor}, \eta_C^*, n_{Ccor}, T_3^*, T_H^*, \eta_i^*, \sigma_i\right),$$

where η_i^*, σ_i – efficiency and recovery factors, respectively, of total pressure suitable for elements of throttling system (combustion chamber, turbines, etc.). The determination of steady-state line point co-ordinates and knowledge of the surge-line co-ordinates on the full compressor map finally enables one to calculate the value of compressor surge margin.

3.1. The algorithm of calculating working line point co-ordinates

From the thermogasdynamical calculations of engine, one knows the location and parameters of the n–th point of the working line, the so called design point, i.e.,

$$Y_{dp} \equiv Y_n = f_n\left(\pi_{Cdp}^*, (G_{1cor})_{dp}, \eta_{Cdp}^*, (n_{Ccor})_{dp}, T_{3\,dp}^*, T_{H\,dp}^*, \eta_{idp}^*, \sigma_{idp}\right).$$

The co-ordinates of this point are plotted on a chosen branch of compressor map for given flight conditions (flight altitude H, free stream static temperature T_H, static pressure p_H, and flight speed V_H). To determine the (n-1) point, one assumes the location of this point on a chosen corrected speed line of compressor map (Fig. 2).

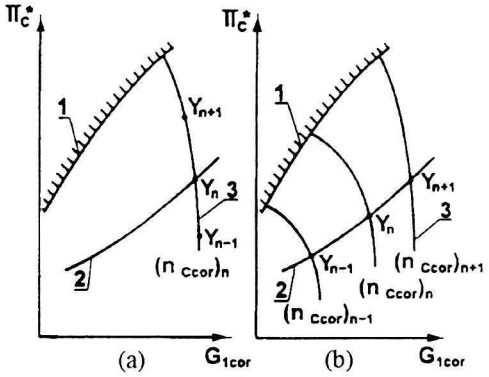

Fig. 2. Illustration of location changes of C-CT working line points for the case when corrected speed n_{Ccor} = idem (a) and speed n_{Ccor} = var (b)

Next, the procedure of calculating the point co-ordinates of operating line is as follows:

- Air stagnation temperature at inlet of compressor

$$T_1^* = T_H^* = T_H\left(1 + \frac{k-1}{2} M_H^2\right), \tag{50}$$

where, flight Mach number

$$M_H = \frac{V_H}{\sqrt{kRT_H}}, \tag{51}$$

- Air stagnation pressure at inlet of compressor

$$p_1^* = \sigma_{IN} p_H^* = \sigma_{IN} p_H \left(1 + \frac{k-1}{2} M_H^2\right)^{\frac{k}{k-1}}, \tag{52}$$

where, total pressure recovery factor of the engine intake

$$\sigma_{IN} = \sigma_{con} \sigma_{sw}. \tag{53}$$

For helicopters, the flight speed is subsonic. Hence, total pressure recovery factor for shock waves system generated at intake σ_{sw}=1 and intake duct total pressure recovery factor (confusor) – σ_{con} [4] is

$$\sigma_{con} = \left(\frac{1 - \frac{k-1}{k+1}\frac{\lambda_1^2}{\varphi_1^2}}{1 - \frac{k-1}{k+1}\lambda_1^2}\right)^{\frac{k}{k-1}}. \tag{54}$$

Absolute velocity loss factor φ_1 and Laval number of absolute velocity for air entering into the compressor λ_1 may be assumed as φ_1=0.95÷0.97; λ_1=0.5÷0.6. The value of σ_{IN} may be also determined on the basis of experimental characteristics of engine intake. In this case, one may find G_{1cor} from the π_C^* on the compressor map and next find σ_{IN} from the intake characteristics $\sigma_{IN} = f(G_{1cor})$.

Because λ_1 and φ_1 vary very weakly, usually a constant value of total pressure recovery factor of the engine intake $\sigma_{IN} = \text{idem}$ is assumed [18].

- Corrected rotational speed of compressor shaft

$$n_{Ccor} = n_C \sqrt{\frac{288.15}{T_1^*}}. \tag{55}$$

- Total pressure ratio of compressor – π_C^*, stagnation isentropic efficiency – η_C^*, and corrected mass flow-rate of air at compressor inlet – G_{1cor} are found from the full compressor map (for given corrected rotational speed).
- Actual mass flow rate of air at compressor inlet

$$G_1 = G_{1cor} \frac{p_1^*}{101325} \sqrt{\frac{288.15}{T_1^*}}. \tag{56}$$

- Average specific heat of air at constant pressure for compressor

$$c_{pa1-2} = \frac{c_{pa2} T_2^* - c_{pa1} T_1^*}{T_2^* - T_1^*}, \tag{57}$$

where: c_{pa1}, c_{pa2} - specific heat of air at constant pressure for compressor inlet and outlet total temperature, respectively.

The value of compressor outlet stagnation temperature – T_2^* is initially assumed.

- Compressor outlet stagnation temperature

$$T_2^* = T_1^* \left(1 + \left(\pi_C^{*\frac{R_a}{c_{pa1-2}}} - 1 \right) \frac{1}{\eta_C^*} \right). \tag{58}$$

If the value of T_2^* differs from the initially assumed value by more than 0.01 K, then the calculations with formulae (57) and (58) are repeated.

- Effective work of compression

$$l_{eC} = c_{pa1-2} \left(T_2^* - T_1^* \right). \tag{59}$$

- Effective power of compressor

$$N_C = G_1 l_{eC}. \tag{60}$$

- Compressor outlet stagnation pressure

$$p_2^* = \pi_C^* p_1^*. \tag{61}$$

- Mass flow rate of air entering the combustion chamber

$$G_{2B} = G_1 (1 - \delta_u), \tag{62}$$

where: δ_u – relative quantity of mass flow rate of air removed from compressor for cooling engine components and for labyrinth seals.

- Mass flux density of air at compressor outlet

$$q(\lambda_2) = \frac{G_{2B}\sqrt{T_2^*}}{s_{fa} p_2^* F_2}, \tag{63}$$

where: F_2 – cross-sectional area of compressor outlet

$s_{fa} = 0.0404$ [J/kgK]$^{-1/2}$.

- Laval number of air at compressor outlet is calculated from the relation

$$q(\lambda_2) = \lambda_2 \left(1 - \frac{k-1}{k+1} \lambda_2^2 \right)^{\frac{1}{k-1}} \left(\frac{k+1}{2} \right)^{\frac{1}{k-1}}. \tag{64}$$

- The value of total temperature of combustion gas at combustor outlet – T_3^* is initially assumed.

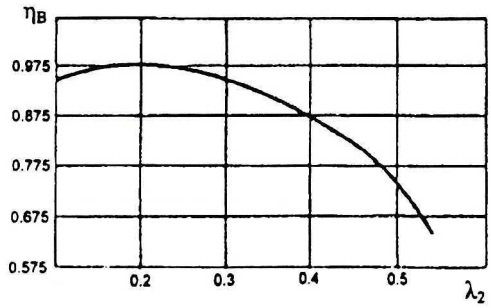

Fig. 3. Combustor efficiency, η_B versus Laval number of absolute velocity at compressor outlet, λ_2

- Overall air excess coefficient at combustor outlet

$$\alpha_3 = \frac{1}{L_t} \frac{\eta_B W_d + T_3^* \left[L_t c_{pa3}\left(T_3^*\right) - \left(1 + L_t\right) c_{ps3}\left(T_3^*, \alpha = 1\right) \right]}{c_{pa3}\left(T_3^*\right) T_3^* - c_{pa2} T_2^*}, \tag{65}$$

where: c_{pa3} – specific heat of air at constant pressure for temperature T_3^*,
c_{ps3} $(T_3^*,\ \alpha = 1)$ – specific heat of stoichiometric combustion gas for temperature T_3^*,
η_B – combustor efficiency,
L_t – stoichiometric air/fuel ratio,
W_d – lower calorific value.

- Total pressure recovery factor at combustion chamber is found from the combustion chamber characteristics

$$\sigma_B = f\left(\lambda_2, \Theta\right), \tag{66}$$

where

$$\Theta = \frac{T_3^*}{T_2^*}.$$

- Total pressure of gas at combustor outlet

$$p_3^* = p_2^* \sigma_B. \tag{67}$$

- Fuel mass flow rate

$$G_f = \frac{G_{2B}}{\alpha_3 L_t} \ [\text{kg/s}]. \tag{68}$$

- Mass flow rate of combustion gas at the outlet of combustion chamber

$$\left(G_{GV}\right)_{CT} = G_{2B} + G_f. \tag{69}$$

- Specific heat of gas at the outlet of combustion chamber

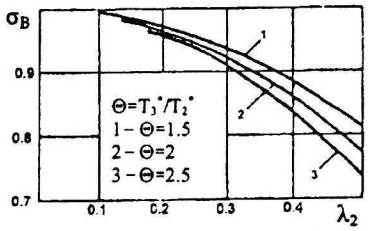

Fig. 4. Total pressure recovery factor at combustion chamber, σ_B versus Laval number of absolute velocity at compressor outlet, λ_2

$$c_{p3}\left(\alpha_3\right) = \frac{\left(1 + L_t\right) c_{ps3}\left(T_3^*, \alpha = 1\right) + L_t\left(\alpha_3 - 1\right) c_{pa3}\left(T_3^*\right)}{\alpha_3 L_t + 1}. \tag{70}$$

- Individual gas constant for combustion gas

$$R(\alpha_3)=\frac{4229.41086\alpha_3+288.700385}{1\ +\ 14.70252\alpha_3}. \tag{71}$$

- Power of compressor turbine

$$N_{CT}=\frac{N_C}{\eta_{mCT}}, \tag{72}$$

where: η_{mCT} – mechanical efficiency of gas producer shafting-line.

- The value of total temperature of combustion gas at gas generator turbine outlet – $T^*_{4'}$ is initially assumed.
- Specific heat of combustion gas at gas generator turbine outlet for a given temperature is calculated by the approximation formula
- Total temperature of combustion gas at gas generator turbine outlet

$$T^*_{4'}=\frac{T^*_3 c_{p3}(\alpha_3)-\dfrac{N_{CT}}{(G_{GV})_{CT}}}{c_{p4'}(\alpha_3)}. \tag{73}$$

If the value of $T^*_{4'}$ differs from the initially assumed value by more than 0.01 K, then the calculations for $c^*_{p4'}(a_3)$ are repeated.

- The decrease of total temperature of gas at compressor turbine

$$\Delta T^*_{CT}=T^*_3-T^*_{4'}. \tag{74}$$

- Average specific heat of combustion gas for compressor turbine

$$C_{p3-4'}=\frac{T^*_3 c_{p3}(\alpha_3)-T^*_{4'}c_{p4'}(\alpha_3)}{\Delta T^*_{CT}}. \tag{75}$$

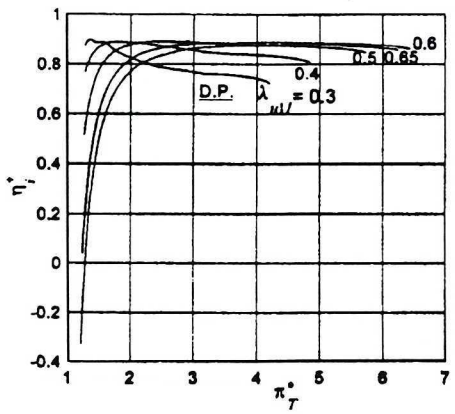

Fig. 5. Compressor turbine efficiency characteristics – isentropic efficiency of gasifier turbine, $\eta_{CT}{}^* = f(\pi_{CT}{}^*, \lambda_{u1})$ versus total pressure ratio for different values of Laval number $\lambda_{u1} = 5{,}786 \cdot 10^{-4}\, n_{CT}/\sqrt{T_3{}^*}$ [3]

- Total pressure ratio of combustion gas at compressor turbine

$$\pi_{CT}^{*} = \frac{1}{\left(1 - \frac{\Delta T_{CT}^{*}}{T_3^{*}\ \eta_{CT}^{*}}\right)^{\frac{c_{p3-4'}}{R(\alpha_3)}}}, \tag{76}$$

where: η_{CT}^{*} – isentropic efficiency of compressor turbine determined from turbine characteristics.

The factor $n_{CT}/\sqrt{T_3^{*}}$ is found for a given n_C and the assumed temperature T_3^{*}. Basing on this factor and π_{CT}^{*}, one determines the value of η_{CT}^{*} and mass flow parameter A_{CT} from the compressor turbine characteristics.

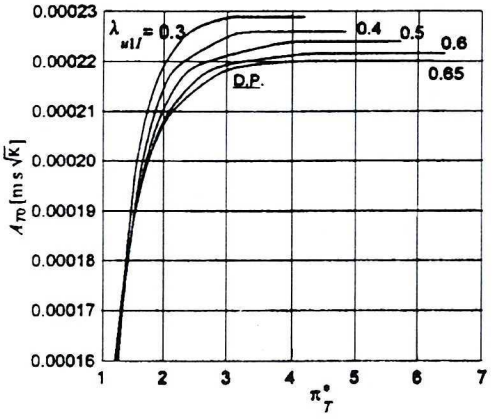

Fig. 6. Characteristics of compressor turbine flow capacity – mass flow parameter of gasifier turbine $A_{CT} = f(\pi_{CT}^{*}, \lambda_{ul})$ versus total pressure ratio for different values of Laval number λ_{ul} [3]

- Total pressure of combustion gas at gas generator turbine outlet

$$p_{4'}^{*} = \frac{p_3^{*}}{\pi_{CT}^{*}}. \tag{77}$$

- Mass flow rate of combustion gas at gas generator turbine inlet

$$(G_{GV})_{CT}^{\cdot} = A_{CT}\frac{p_3^{*}}{\sqrt{T_3^{*}}}. \tag{78}$$

If $(G_{GV})'_{CT} = (G_{GV})_{CT}$ the calculations are continued. If $\left|(G_{GV})'_{CT} - (G_{GV})_{CT}\right| > 0.5\%$, then new temperature T_3^{*} is assumed higher than the previously assumed temperature T_3^{*} (when $(G_{GV})_{CT}{}' > (G_{GV})_{CT}$) and the calculations are repeated for formulas from (65) to (78).

- Total pressure of combustion gas at turbine power inlet

$$p_4^{*} = p_{4'}^{*}\sigma_{MT}, \tag{79}$$

where: σ_{MT} – total pressure loss recovery factor at the connecting channel between compressor turbine and power turbine.

- Combustion gas mass stream entering the power turbine

$$(G_{GV})_{PT} = (G_{GV})_{CT} + \delta_{PT} G_1, \tag{80}$$

where: δ_{PT} – relative cooling of air mass stream going back to power turbine flow duct.

- Air excess coefficient of combustion gas at power turbine inlet

$$\alpha_4 = \alpha_3 \left(1 + \frac{\delta_{PT} G_1}{G_{2B}} \right). \tag{81}$$

- The value of total temperature of combustion gas at power turbine inlet – T_4^* is initially assumed.
- Specific heat of stoichiometric combustion gas c_{ps4} (T_4^*, $a_4 = 1$) is calculated for the assumed temperature T_4^*.
- Specific heat of air c_{pa4} (T_4^*) is calculated for the assumed temperature T_4^*.
- Specific heat of actual gas entering to power turbine

$$c_{p4}(\alpha_4) = \frac{(1 + L_t) c_{ps4}(T_4^*, \alpha_4 = 1) + (\alpha_4 - 1) c_{pa4}(T_4^*) L_t}{1 + \alpha_4 L_t}. \tag{82}$$

- Total temperature of combustion gas at power turbine inlet

$$T_4^* = \frac{c_{p4'}(\alpha_3) T_4^* (G_{GV})_{CT} + \delta_{PT} G_1 c_{p2} T_2^*}{(G_{GV})_{PT} c_{p4}(\alpha_4)}. \tag{83}$$

If the value of temperature T_4^* differs from the initially assumed value by more than 0,01 K, then the calculations for $c_{p4}(\alpha_4)$ are repeated.

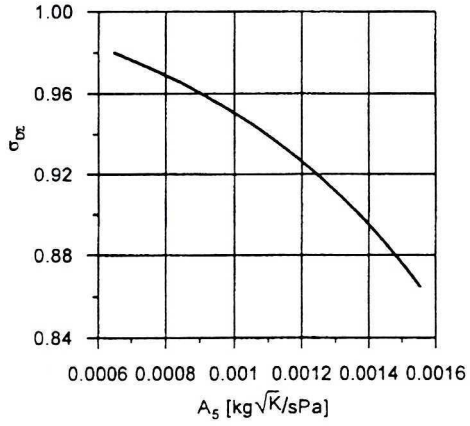

Fig. 7. Exhaust diffuser characteristic – pressure ratio $\sigma_{D\Sigma} = p_H/p_5^*$ versus mass flow parameter at diffuser inlet $A_5 = (G_{GV})_{PT} \sqrt{T_5^*}/p_5^*$ [6]

- Individual gas constant for combustion gas at power turbine

$$R(\alpha_4) = \frac{4220.41086\alpha_4 + 288.700385}{1 + 14.70252\alpha_4}. \tag{84}$$

- Total pressure of combustion gas at power turbine outlet

$$p_5^* = \frac{p_H}{\sigma_{D\Sigma}}, \tag{85}$$

where: $\sigma_{D\Sigma}$ – exhaust diffuser pressure ratio is found from the characteristic $\sigma_{D\Sigma} = f(A_5)$.

- Total pressure ratio of combustion gas for power turbine

$$\pi_{PT}^* = \frac{p_4^*}{p_5^*}. \tag{86}$$

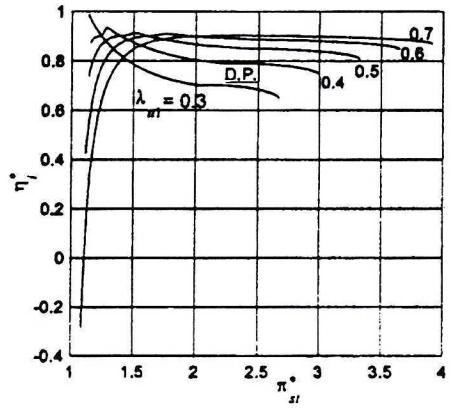

Fig. 8. Power turbine efficiency characteristics – isentropic efficiency of power turbine $\eta_{PT}^* = f(\pi_{PT}^*, \lambda_{ul})$ versus pressure ratio for different values of Laval number $\lambda_{ul} = 6{,}215 \cdot 10^{-4}\, n_{PT}/\sqrt{T_4^*}$ [3]

- Isentropic efficiency of power turbine η_{PT}^* is determined from characteristics basing on the factor $n_{PT}/\sqrt{T_4^*}$ and π_{PT}^*. The value of mass flow parameter A_{PT} is similarly determined from the power turbine characteristics.
- Mass flow rate of combustion gas at power turbine inlet

$$(G_{GV})_{PT}' = A_{PT} \frac{p_4^*}{\sqrt{T_4^*}}. \tag{87}$$

If $(G_{GV})_{PT}' = (G_{GV})_{PT}$, the calculations are continued. If $\left|(G_{GV})_{PT}' - (G_{GV})_{PT}\right| > 0.5\%$, then new temperature T_3^* is assumed and the calculations are repeated for new values of compressor ratio π_C^*, isentropic efficiency of compressor η_C^*, and mass flow rate of air at compressor inlet G_{1cor}.

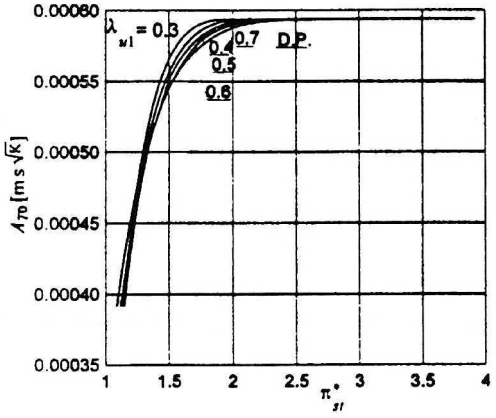

Fig. 9. Characteristics of power turbine flow capacity – mass flow parameter of power turbine $A_{PT} = f(\pi_{PT}^*, \lambda_{u1})$ versus total pressure ratio for different values of Laval number λ_{u1} [3]

If $(G_{GV})'_{PT} < (G_{GV})_{PT}$, then a point of higher compression ratio shall be taken on a chosen branch of compressor map.

- The value of total temperature of combustion gas at power turbine outlet – T_5^* is initially assumed.
- Specific heat of combustion gas $c_{p5}(\alpha_5)$ is calculated for the assumed temperature T_5^*, but $\alpha_5 = \alpha_4$.
- Average specific heat of combustion gas for power turbine.

$$c_{4-5} = \frac{c_{p4}(\alpha_4)T_4^* - c_{p5}(\alpha_4)T_5^*}{T_4^* - T_5^*}. \tag{88}$$

- Total temperature of gas at power turbine outlet

$$T_5^* = T_4^*\left(1-\eta_{PT}^*\right)\left(1-\frac{1}{\pi_{PT}^{*\frac{R(\alpha_4)}{c_{p4-5}}}}\right) \tag{89}$$

- Effective power

$$N_{PT} = (G_{GV})_{PT}\left(c_{p4}(\alpha_4)T_4^* - c_{p5}(\alpha_4)T_5^*\right). \tag{90}$$

- Output shaft power of engine

$$N_e = \frac{N_{PT}\eta_{mPT}\eta_{RED}}{1000}\ [\mathrm{kW}], \tag{91}$$

where: η_{mPT} – mechanical efficiency of power turbine, η_{RED} – reduction gear efficiency. For gearless engine, $\eta_{RED} = 1$.

- Fuel flow

$$G_f^h = 3600 G_f\ [\mathrm{kg/h}]. \tag{92}$$

- Shaft power specific fuel consumption

$$c_e = \frac{G_f^h}{N_e} \quad [\mathrm{kg/kWh}]. \tag{93}$$

- Compressor stable running factor

$$K_C = \frac{\pi^*_{Csl}/(G_{1cor})_{sl}}{\pi^*_C/G_{1cor}}.$$

- Surge margin of compressor

$$\Delta K_{S\%} = (K_S - 1)\cdot 100, \quad \%.$$

4. Criteria applied to the correction of engine parameters during determining the co-ordinates of C-CT working line points

The determination of the co-ordinates of C-CT working line points, according to the sequence algorithm as described in the section 3.1, requires full thermogasdynamics calculations of turboshaft engine [4], [15] for defined geometry of the flow duct. However, the input data for calculations are not known: compressor pressure ratio, corrected mass flow rate at compressor inlet, and total temperature of combustion gas at combustor outlet. While calculating the co-ordinates of C-CT working line, we know the position of the n-th point on the operating line, $Y_n = Y_{dp}$, called the design point, Fig. 2. The co-ordinates of the next point on the operating line (Y_{n-1} or Y_{n+1}) may be found by the method of successive approximations taking into consideration variability of efficiencies of the assembly: $\eta^*_B, \eta^*_{CT}, \eta^*_{PT}$ and recovery factors of total pressure: σ_B and $\sigma_{IO\Sigma}$.

By initially assuming the co-ordinates of working line point calculated on the full compressor map, one determines the tarting parameters of engine compressors: $(\pi^*_C)_{n-1}$, $(G_{icor})_{n-1}$, $(\eta^*_C)_{n-1}$. Next, the value of stagnation temperature at compressor turbine inlet T_3^* and the efficiencies of remaining engine assemblies are assumed. Having done the first approximation, the η^*_{CT} value is corrected on the basis of the compressor turbine efficiency characteristics. Next, the condition of turbine flow capacity is checked, i.e., the gas flow rate at gas generator turbine inlet is checked for conformity with the gas flow rate obtained from combustion chamber calculations.

In the case when the mentioned above gas flow rates are not equal, the value of T_3^* is corrected according to the formula

$$\left(T_3^*\right)_{j+1} = \left(A_{CT} \frac{p^*_{3j}}{(G_{GV})_{CTj}} \right)^2 \tag{94}$$

where: A_{CT} – mass flow parameter determined from the compressor turbine characteristics, j – number of successive approximation.

If the result of checking of power turbine flow capacity is negative, it is necessary to change the value of co-ordinates of steady-state operating line on

the corrected speed branch, $n_{Ccor} = \text{idem}$, of compressor map. Thus, if the gas flow rate at power turbine inlet is greater than the gas flow rate $(G_{GV})'_{CT}$ calculated from the flow capacity formula (equation 78), then the point of C-CT operating line moves in the direction of the surge limit. This effect causes a decrease of the corrected mass flow rate of air at the compressor inlet G_{1cor} and an increase of compressor pressure ratio π_C^*, and a change of stagnation isentropic efficiency η_C^*. Because the values of G_{1cor}, π_C^* and η_C^* are changed, this situation requires that calculations should be repeated with the algorithm presented in section 3.1 with suitable corrections of efficiencies of all engine assemblies. The procedure shown above has been applied for the case $n_{Ccor} = \text{var}$. It should be emphasised that during successive approximations in calculations of co-ordinates of C-CT working line points it is necessary to fulfil the flow similarity criteria in adequate assemblies of turboshaft engine [2]. A list of flow similarity criteria used for different cases of calculations of co-ordinates of C-CT working line points of PZL-10W2 turboshaft engine, obtained from the Report [5], is presented in Table 1.

Table 1.

Flow similarity criteria of turbine nozzle rims of the PZL-10W2 turboshaft engine

Criterion formula	Case of counting			Design point value	Unit
	n_{Ccor} =idem $(F_{GV})_{PT}$ =idem $(F_{GV})_{CT}$ =var	n_{Ccor} = idem $(F_{GV})_{PT}$ =var $(F_{GV})_{CT}$ =idem	n_{Ccor} =var $(F_{GV})_{PT}$ =idem $(F_{GV})_{CT}$ =idem		
$\bar{A}_{PT} = \dfrac{(G_{GV})_{PT}\sqrt{T_4^*}}{(F_{GV})_{PT}\, p_4^*} = \text{idem}$	No	Yes	No	$3{,}9603 \cdot 10^{-2}$	$\dfrac{\text{kg}\sqrt{\text{K}}}{\text{sN}}$
$A_{CT} = \dfrac{(G_{GV})_{CT}\sqrt{T_3^*}}{p_3^*} = \text{idem}$	No	Yes	Yes	$2{,}2341 \cdot 10^{-4}$	$\dfrac{\text{kg}\sqrt{\text{K}}}{\text{sPa}}$
$A_{PT} = \dfrac{(G_{GV})_{PT}\sqrt{T_4^*}}{p_4^*} = \text{idem}$	Yes	No	Yes	$5{,}9009 \cdot 10^{-4}$	$\dfrac{\text{kg}\sqrt{\text{K}}}{\text{sPa}}$
$\bar{A}_{CT} = \dfrac{(G_{GV})_{CT}\sqrt{T_3^*}}{(F_{GV})_{CT}\, p_3^*} = \text{idem}$	Yes	No	No	$3{,}6903 \cdot 10^{-2}$	$\dfrac{\text{kg}\sqrt{\text{K}}}{\text{sN}}$

Actions of correction of engine parameters during determining the co-ordinates of C-CT operating line points on compressor map for the case $n_{Ccor} = \text{idem}$ are similar as those in the case presented above $n_{Ccor} = \text{var}$ with the following differencies:

- For the variant $(F_{GV})_{CT} = \text{idem}$, $(F_{GV})_{PT} = \text{var}$, stagnation temperature of combustion gas at compressor turbine inlet is determined by relation (94).

Minimal section area of power turbine guide vanes is determined by the formula

$$(F_{GV})_{PTj} = \frac{A_{PTj}}{A_{PTdp}}, \tag{95}$$

- for the variant $(F_{GV})_{CT} = \text{var}$, $(F_{GV})_{PT} = \text{idem}$, stagnation temperature of combustion gas at compressor turbine inlet is determined by the relation

$$T^*_{3\,j+1} = \left(\frac{A_{PTdp}\, p^*_{4\,j}}{(G_{GV})_{PTj}} \right)^2 + \delta T^*_{MT} + \Delta T^*_{CT}, \tag{96}$$

where

$$\delta T^*_{MT} = T^*_{4'\,j} - T^*_{4\,j}, \tag{97}$$

$$\Delta T^*_{CT} = T^*_{3\,j} - T^*_{4'\,j}. \tag{98}$$

Throat area of compressor turbine nozzle diaphragm is calculated from the equation

$$(F_{GV})_{CTj} = \frac{A_{CTj}}{A_{CTdp}} \tag{99}$$

5. Conclusions

The analytical (section 2) and numerical methods (section 3) of calculating the surge margin of the compressor, presented in this paper, may be used for super-critical, critical, and sub-critical pressure ratios in engine turbine stages, i.e., when Laval number of absolute velocity at outlet nozzle diaphragm $\lambda_{C1} \geq 0.9$.

WSK „PZL-Rzeszów" S.A. has elaborated its original analytical and numerical method to determine the influence of $(F_{GV})_{PT}$ and $(F_{GV})_{CT}$ on the compressor surge margin value of turboshaft engine with free power turbine for the case $n_{Ccor} = \text{idem}$, and has made a number of experimental tests [5], [7]. Reduction of test costs was obtained by adjusting the minimal section area of power turbine nozzle rim by bending trailing edges and for compressor turbine by changing vane chord length (grinding of trailing edges).

The comparison of values $\Delta(\pi^*_C / G_{1cor})$ obtained by analytical and numerical method and the values found experimentally is presented in Fig. 10 for the case $n_{Ccor} = \text{idem}$ [5].

Analysing the course of $\Delta(\pi^*_C / G_{1cor})$ ratio one may state that the values calculated with the analytical method are slightly greater than the ones obtained with the numerical method and greater then the experimental ones. However, it should be emphasised that the relations (28) and (48) are essentially significant, because they make it possible to quickly determine changes of $\Delta(\pi^*_C / G_{1cor})$ ratios with an accuracy satisfactory for engineering practise. For small changes of $\Delta(F_{GV})_{CT}$ and $\Delta(F_{GV})_{PT}$, the results obtained from equations (28) and (48)

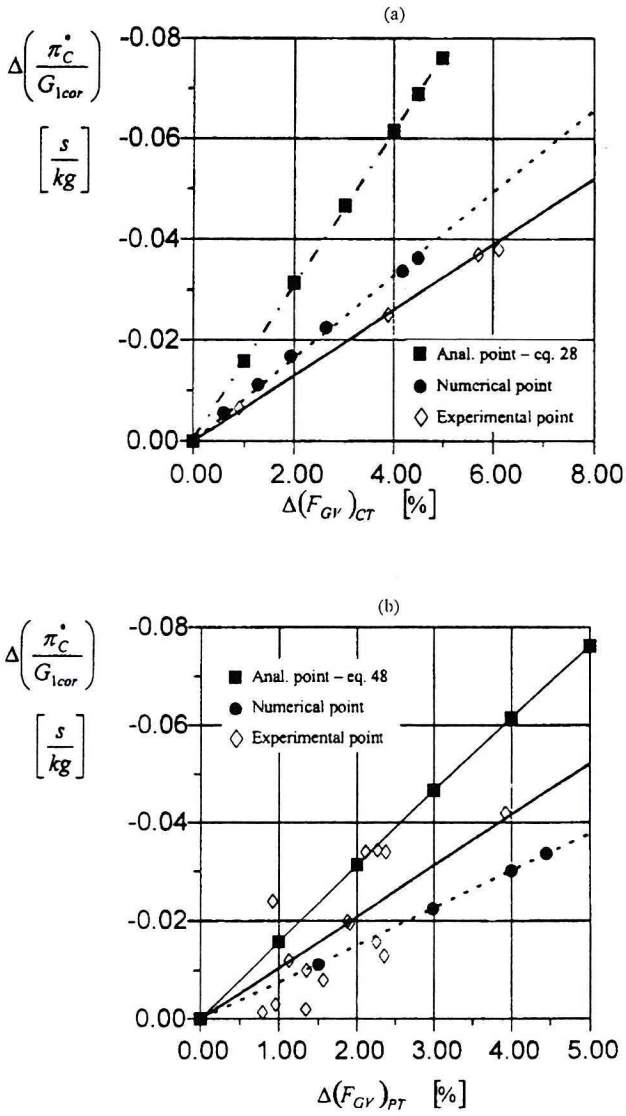

Fig. 10. Effect of minimal section area increase of gasifier (a) and power (b) turbine nozzle rim on decrease of the value $\Delta(\pi_C^*/G_{1cor})$

are satisfactory, because in manufacturing conditions they are usually within a limit of 0,5 – 2%. It should be stated that these equations are of universal nature, and they are valid for all turboshaft engines whose characteristics are close to those of circumcritical flow in gasifier and power turbines diaphragm. It should be noted that relations (28) and (48) are especially useful for designers, when there are no experimental results expressing the influence of geometrical parameters of turbine nozzle diaphragm on the engine performance, and hence,

compressor surge margin that must be known in the preliminary design. The usage of relations (28) and (48) is very convenient. However, a better accuracy in calculating changes of $\Delta(\pi_C^* / G_{1cor})$ ratio may be easily obtained by adding correction factors

$$\Delta\left(\frac{\pi_C^*}{G_{1cor}}\right)_{real} = (eq.28) - k_{CT}\Delta(F_{GV})_{CT} \tag{100}$$

$$\Delta\left(\frac{\pi_C^*}{G_{1cor}}\right)_{real} = (eq.48) - k_{PT}\Delta(F_{GV})_{PT} \tag{101}$$

The values of correction factors k_{PT} and k_{CT} are selected in such a way that the values from semi-empirical equations (100) and (101) are as close as possible to the values obtained from experiments. For PZL-10W2 turboshaft engine k_{PT} = -0.00475 and k_{CT} = -0.0085.

The results presented in Fig. 10 and equation (28) and (48), to the best of author's knowledge, are published for the first time.

The numerical method of calculating the co-ordinates of C-CT working line points and compressor surge margin is given in section 3. It is based on sequential solving of equations describing operation of turboshaft engine with free power turbine in the conditions of thermogasdynamic equilibrium of working medium flow. The characteristics of engine assemblies are also taken into consideration.

An inverse algorithm of calculating working line parameters for a turbojet engine is presented in the article [1], [20]. Approximation formulas for actual specific heat for air and combustion gas are not included, in order to increase clarity of the numerical algorithm.

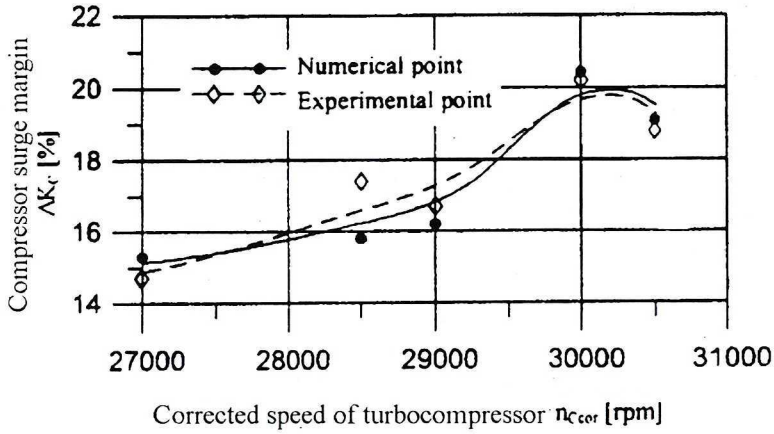

Fig. 11. Compressor surge margin versus corrected speed of turbocompressor of the turboshaft engine PZL-10W2

The comparison of surge margin values obtained by the numerical method and values found experimentally is presented in Fig. 11 for the case $n_{Ccor} = \text{var}$. It should be underlined that the calculated course of $\Delta K_{C\%}$ approximates experimental results with a satisfactory accuracy within the range of the analysed compressor speed.

It should be added that the analytical and numerical methods of calculating the surge margin of the compressor, presented in this article, require that the map of full compressor, calculated or experimentally determined must be initially known [9], [10], [11], [17].

Manuscript received by Editorial Board, July 05, 2001;
final version, November 20, 2001.

REFERENCES

[1] Akhmedzyanov D.A., Gumerov Kh.C., Ivanov I.V.: Simple and inverse method of calculating of transient regimes for gas turbine engines. Izvestiya Vysshikh Uchebnykh Zavedenii, Aviatsionnaya Tekhnika, No. 3, 1996, pp. 86÷90 (In Russian).

[2] Antas S.: The selection of turbine critical parameters for providing stable compressor operation range. The Archive of Mechanical Engineering, Vol. XLVI, No. 3, 1999, pp. 273÷299.

[3] Antas S., Chmielniak T., Kujda J.: A method for the calculation of characteristics of one-stage and two-stage axial flow turbines. The Transactions Institute of Fluid-Flow Machinery, No. 2, 2001 (In the press).

[4] Antas S., Wolański P.: Thermogasdynamic Calculation of Aviation Turbine Engines. Publishing House of Warsaw University of Technology, Warsaw 1989, pp. 196 (In Polish).

[5] Antas S.: Analysis of compressor surge margin for PZL-10W2 turboshaft engine. Doc. No. 19.0.915, WSK "PZL-Rzeszów" S.A., 2001, pp. 85 (In Polish).

[6] Antas. S., Kujda J.: Conceptual design study of PZL-10W engine with increased Take-off power up to 1000 HP. WSK "PZL-Rzeszów" S.A., Doc. No. 19.0.470, 1997, pp. 101 (In Polish).

[7] Antas S. [et al.]: Technical design of PZL-10W engine with increased Take-off power up to 1000 HP. Part I, Flow Counting and Experimental Tests, WSK "PZL-Rzeszów" S.A., Doc. No. 19.0.908, 2000, pp.454.

[8] Benser W.A., Finger H.B.: Compressor stall problems in gas-turbine-type aircraft engines. SAE Transactions, Vol. 65, 1957, pp. 187÷200.

[9] Cai Yuan-Hu [et al.]: A new method for predicting performance of axial-flow compressor. International Journal of Turbo and Jet Engines. Vol. 12, 1995, pp. 21÷28.

[10] Elaraby M., Mobarak A., Shash Y.: Turbocompressor surge and surge control. AIAA Paper, No. 70, 1981, pp. 9.

[11] El-Gammal A.M.: An algorithm and criteria for compressor characteristics real time modeling and approximation. Transactions of the ASME, Journal of Engineering for Gas Turbines and Power, Vol. 113, 1991, pp. 112÷118.

[12] Emmons H.W., Pearson C.E., Grant H.P.: Compressor surge and stall propagation. Transactions of the ASME, Vol. 79, 1955, pp. 455÷469.

[13] Greitzer E.M.: Surge and rotating stall in axial flow compressors: Part I. Theoretical Compressor System Model. Transactions of the ASME, Journal of Engineering for Power, Vol. 98, 1976, pp. 190÷198.

[14] Hendricks G.J., Sabnis J.S., Feulner M.J.: Analysis of instability inception in high-speed multistage axial-flow compressors. Transactions of the ASME, Journal of Turbomachinery, Vol. 119, 1997, pp. 714÷722.

[15] Ismail I.H., Bhinder F.S.: Simulation of aircraft gas turbine engines. Transactions of the ASME, Journal of Engineering for Gas Turbines and Power, Vol. 113, 1991, pp. 95÷99.

[16] Oakes W., Shook P., McGuire R., Fleeter S.: Aerodynamic performance and instability initiation of a high speed research centrifugal compressor. International Journal of Turbo and Jet Engines, Vol. 14, 1997, pp. 187÷199.

[17] Raw J.A., Weir G.C.: The prediction of off-design characteristics of axial and axial/centrifugal compressors. SAE Techn. Pap. Ser., 1980, No. 800628, pp. 11÷19.

[18] Sanghi V., Sane S.K.: Digital simulation of propulsion system performance for cycle optimization studies. International Journal of Turbomachinery, Vol. 16, 1999, pp. 27÷37.

[19] Spakovszky Z.S. [et al.]: Influence of compressor deterioration on engine dynamic behavior and transient stall margin. Transactions of the ASME, Journal of Turbomachinery, Vol. 122, 2000, pp. 477÷484.

[20] Wang Y.: A New method of predicting the performance of gas turbine engines. Transactions of the ASME, Journal of Engineering for Gas Turbines and Power, Vol. 113, 1991, pp. 107÷111.

Metoda analityczna i numeryczna obliczania zapasu statecznej pracy sprężarki silnika śmigłowcowego z wolną turbiną napędową

Streszczenie

Praca obejmuje opis wszechstronnej analizy teoretycznej prowadzonej w celu zapewnienia zakresu statecznej pracy sprężarki. W artykule przedstawiono obliczenia wartości zapasu statecznej pracy sprężarki, wykonane przy użyciu opracowanych przez autora oryginalnych metod analitycznej i numerycznej. Metodą analityczną i numeryczną określono wpływ zmian przekroju minimalnego wieńca dyszowego turbiny wytwornicowej $(F_{GV})_{CT}$ i turbiny napędowej $(F_{GV})_{PT}$ na zapas statecznej pracy sprężarki mierzony w warunkach produkcyjnych wartością wskaźnika π_C^*/G_{1cor}. Rezultaty badań teoretycznych zweryfikowano parametrami zmierzonymi, uzyskanymi podczas badań eksperymentalnych silnika śmigłowcowego z wolną turbiną napędową. W zakończeniu pracy przedstawiono wnioski wynikające z porównania wyników badań teoretycznych i eksperymentalnych.